

BESIII $\pi^+\pi^-$ form factor measurement and perspective of $\pi^+\pi^-\pi^0$

WANG Yaqian (for the BESIII Collaboration)

(Johannes-Gutenberg University, Mainz 55128, Germany)

Abstract: The cross section is measured of $e^+e^- \rightarrow \pi^+\pi^-$ in the energy range between 600 and 900 MeV/ c^2 with a 2.93 fb $^{-1}$ data set taken at the center-of-mass energy 3.773 GeV at BESIII. The initial state radiation technique is used, and the total systematic uncertainty is estimated to be 0.9%. The squared form factor $|F_\pi|^2$ is extracted, and comparisons are made with results from both KLOE and BaBar. The two-pion contribution to the hadronic vacuum polarization contribution to $(g-2)_\mu$ is calculated to be $a_\mu^{\pi\pi, LO}(600\sim 900 \text{ MeV}/c^2) = (368.2 \pm 2.5_{\text{stat}} \pm 3.3_{\text{sys}}) \times 10^{-10}$.

Key words: muon anomalous magnetic moment $g-2$; vacuum polarization; initial state radiation (ISR)

CLC number: O572.3 **Document code:** A doi:10.3969/j.issn.0253-2778.2016.04.007

Citation: WANG Yaqian. BESIII $\pi^+\pi^-$ form factor measurement and perspective of $\pi^+\pi^-\pi^0$ [J]. Journal of University of Science and Technology of China, 2016, 46(4): 301-307.

BESIII $\pi^+\pi^-$ 形状因子测量以及 $\pi^+\pi^-\pi^0$ 展望

王亚乾(BESIII 合作组)

(美因茨大学, 美因茨 55128, 德国)

摘要: 利用 BESIII 在 3.773 GeV 获取的 2.93 fb $^{-1}$ 数据, 测量了 600~900 MeV/ c^2 区间 $e^+e^- \rightarrow \pi^+\pi^-$ 的截面. 分析主要基于初态辐射的方法, 总的系统误差控制在 0.9%. 通过计算得到的形状因子 $|F_\pi|^2$ 与其他两个实验做了比较. 两 π 过程对缪子反常磁矩的贡献为 $a_\mu^{\pi\pi, LO}(600\sim 900 \text{ MeV}/c^2) = (368.2 \pm 2.5_{\text{stat}} \pm 3.3_{\text{sys}}) \times 10^{-10}$.

关键词: 缪子反常磁矩; 真空极化; 初态辐射

0 Introduction

The hadronic vacuum polarization (VP) plays an important role in the precision test of the Standard Model (SM). One of the cases is the

theoretical prediction for the anomalous magnetic moment of muon, $a_\mu \equiv (g-2)_\mu/2$. With dozens of years' efforts, the precision on the a_μ is in the order of 6×10^{-10} for both experiment and theory. The significance of the discrepancy of (28.7 ± 8.0)

Received: 2015-11-30; **Revised:** 2016-04-20

Foundation item: Supported by German Research Foundation DFG under Collaborative Research Center (CRC-1044).

Biography: WANG Yaqian, male, born in 1984, PhD. Research field: particle physics. E-mail: whyaqm@gmail.com

$\times 10^{10}$ between them is $3.6\sigma^{[1]}$. In the following years, a new experiment at Fermilab is expected to reach the precision of 0.14 parts per million^[2], which makes the theoretical calculation of a_μ under pressure to improve the precision accordingly.

The largest contribution to a_μ is from quantum electro-dynamics (QED) including all photonic and leptonic loops, and the calculation is performed up to 4-loop level and estimated to 5-loop level. As a result, the error from QED is negligible. The weak part includes Z , W^\pm and Higgs loop contributions, and is suppressed due to the heaviness of their masses. Until now, it is not possible to calculate the hadronic contributions from first principles. Generally, there are three parts in the hadronic contribution. In terms of uncertainty, the largest contribution is from the lowest order (LO) hadronic VP, to a less extent, from the hadronic light-by-light scattering contribution and higher order hadronic VP.

By using the experimental measurements, the hadronic VP contribution is obtained via the dispersion integral^[3-4],

$$a_\mu^{\text{had,LO}} = \frac{\alpha^2(0)}{3\pi^2} \int_{4m_\pi^2}^{\infty} ds \frac{K(s)}{s} R(s) \quad (1)$$

where $K(s)$ is the QED kernel^[5], and $R(s)$ denotes the ratio of the bare cross section for e^+e^- annihilation into hadrons to the point-like muon-pair cross section. The integrand decreases monotonically with increasing s . Therefore, precision measurement at low energy is very important. About 91% of the total contribution to $a_\mu^{\text{had,LO}}$ is accumulated at center-of-mass energies $\sqrt{s} < 1.8$ GeV and the two-pion channel contributes more than 70% of $a_\mu^{\text{had,LO}}$.

Two precision measurements of $\sigma_{\pi\pi}$ have been done by the KLOE Collaboration in Frascati^[6-9], and the BABAR Collaboration at SLAC^[10], both of which claim an accuracy of better than 1% in the energy range below 1 GeV. However, a discrepancy of approximately 3% on the peak of the $\rho(770)$ resonance is observed. The discrepancy is even increasing towards higher energies and has

a large impact on the SM prediction of a_μ .

In this paper, I report the two-pion cross section in the mass range between 600 and 900 MeV/ c^2 . This range includes the important ρ peak, which contributes more than 70% to the two-pion contribution $a_\mu^{\pi\pi}$ and to about 50% of the total hadronic vacuum polarization correction of a_μ . Besides the $\pi^+\pi^-$ channel, perspective on the study of $e^+e^- \rightarrow \pi^+\pi^-\pi^0$ is also included.

1 BESIII experiment

Located at the double-ring Beijing Electron-Positron Collider, the cylindrical BESIII detector covers 93% of the full solid angle. As a multi-functional detector, it is described in detail elsewhere^[12]. A charged-particle tracking system, Multilayer Drift Chamber (MDC), is immersed in a 1 T magnetic field. A time-of-flight (TOF) system and an electromagnetic calorimeter (EMC) surrounding the tracking system are used to identify charged particles and to measure neutral particle energies, respectively. Located outside the EMC, a muon chamber (MUC) is used to detect muon tracks.

2 Cross section measurement

From the integrand of the dispersion integral, the most important contribution comes from the low energy region. We exploit the initial state radiation (ISR) technique to measure the cross section with data sample taken at the 3.773 GeV.

2.1 ISR technique

The emission of the ISR photon is suppressed by $\frac{\alpha}{\pi}$. This is the reason why it is necessary to have large data sample for the application of the ISR technique. Radiation of a high energy photon from the initial e^+ or e^- allows the production of the hadronic system at an energy point ($\sqrt{s'}$) much below the nominal machine energy (\sqrt{s}), which follows $\sqrt{s'} = \sqrt{s - 2\sqrt{s}E_\gamma}$, where E_γ is the energy of the ISR photon. The radiation function, used to

describe this ISR effect, is precisely known. Monte Carlo (MC) samples are available for many channels with PHOKHARA^[13]. The ISR photons favor large polar angles, which is beyond the acceptance of the common symmetrical e^+e^- collider. There is only a small fraction of the ISR photons that falls in the coverage of EMC. In the final state of an ISR event, there are particles including the ISR photon and the hadrons, which should be of course reconstructed to measure the hadronic cross sections. Then, according to the angular direction of the ISR photon, different methods can be used.

If the ISR photon is emitted at small polar angle, it is possible to detect (tag) it, and the ISR event can be fully reconstructed together with the hadronic particles. In this case, a wide mass spectrum is available from threshold to the machine energy. The disadvantage is that we suffer from a large background contribution, especially in the higher mass range.

Since the majority of the ISR photons favor the beam direction, the detector loses the power to find it (untag). It is still possible to reconstruct all the hadronic particles in the ISR events when the energy of the ISR photon is not extremely high. With this characteristic, requiring a missing photon along the beam pipe removes quite an amount of continuum backgrounds and keeps the signal almost background free.

2.2 Measurement of $e^+e^- \rightarrow \pi^+\pi^-$

There are only two charged tracks in the channel under study. As a result, Bhabha events survive the selections due to a very high cross section. Information from dE/dx , TOF and EMC is used to veto electrons and positrons. A 4-constraint (4C) kinematic fit is performed by exploiting the kinematics. Events with χ_{4C}^2 larger than 60 are rejected.

2.2.1 $\mu\pi$ separation

In terms of background level, the most important one is $e^+e^- \rightarrow \gamma\mu^+\mu^-$, in which the kinematics is quite similar to the signal. We utilize

a track-based particle identification (PID), which is based on the artificial neural network (ANN) method, as provided by the TMVA package^[14]. The following observables are exploited for the separation; the Zernicke moments^[15] of the EMC clusters induced by pion or muon tracks, the ratio of the energy E of the charged track deposited in the EMC to its momentum p measured in the MDC, the ionization energy loss dE/dx in the MDC, and the depth of a track in the MUC. The ANN is trained by using MC samples of $\pi^+\pi^-\gamma$ and $\mu^+\mu^-\gamma$. We choose the implementation of a Clermont-Ferrand Multilayer Perceptron (CFMlp) ANN as the method resulting in the best background rejection for a given signal efficiency. The output likelihood y_{ANN} is calculated after training the ANN for the signal pion tracks and background muon tracks. The response value y_{ANN} is required to be greater than 0.6 for each pion candidate in the event selection, yielding a background rejection of more than 90% and a signal loss of less than 30%.

2.2.2 QED test

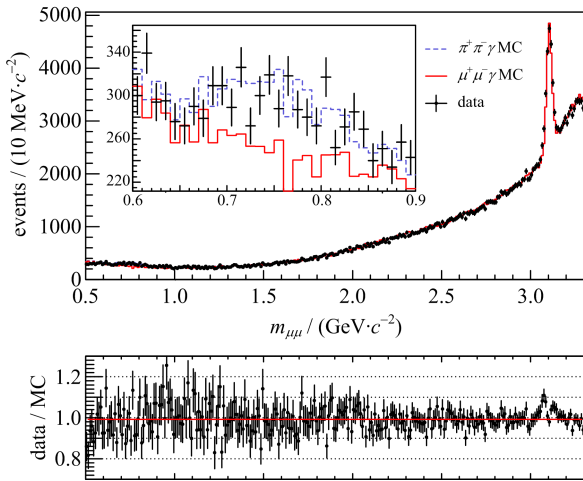
Differences between data and MC are taken to correct the efficiency at the track level. The validity of such corrections needs to be proved.

We select $\mu^+\mu^-\gamma$ events from data and compare them after efficiency corrections with the QED prediction, which is scaled to the luminosity of data. The event selections are quite similar to that for $\pi^+\pi^-\gamma$. The only difference is the PID, i. e., we are selecting muons instead of pions. Fig. 1 shows the comparison of the di-muon mass spectrum between data and QED prediction.

The difference between them is $(1.0 \pm 0.3 \pm 0.9)\%$ from a linear fit as shown below. The uncertainties of the corrections are taken as the systematics, which is 0.9% in total.

2.2.3 Cross section and form factor

With the QED test in the previous section, all the corrections we made to the efficiency prove to be reliable. The cross section is obtained by dividing the two-pion mass spectrum by the global



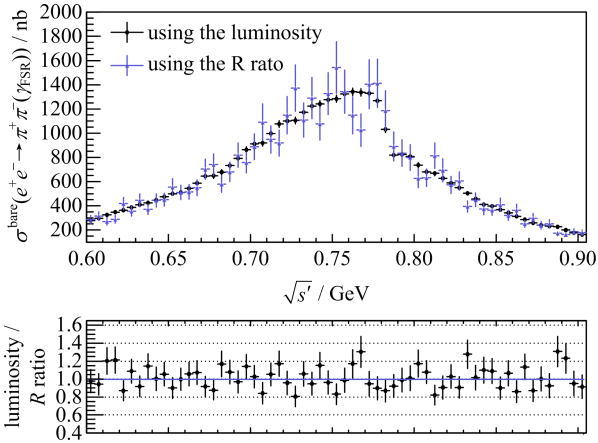
The upper panel presents the event yield found in data and MC.

The inlay shows the zoom for invariant masses between 600 and 900 MeV/c².

The lower panel shows the ratio of these two histograms.

Fig. 1 Invariant $\mu^+ \mu^-$ mass spectrum of data and $\mu^+ \mu^- \gamma$ MC

efficiency and the effective luminosity including corrections of final state radiation (FSR) and VP. The black dots in Fig. 2 show the cross section from 600 to 900 MeV/c².

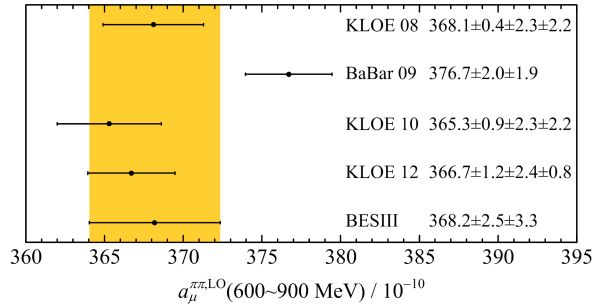


Only the statistical errors are shown.

Fig. 2 The bare $e^+ e^- \rightarrow \pi^+ \pi^- (\gamma_{\text{FSR}})$ cross section

Another method to obtain the cross section is to normalize the $\pi^+ \pi^- \gamma$ events to the $\mu^+ \mu^- \gamma$ events, since the di-muon cross section is precisely known. In this approach, part of the systematics is canceled, for instance, the luminosity, tracking efficiency, photon efficiency, and so on. As shown in Fig. 2, the cross section with this normalization

method, represented as blue dots, shows very good consistency with the black one with a difference estimated to be $(0.85 \pm 1.68)\%$ from a linear fit. Since the precision of the blue dots is limited by the statistics of the $\mu^+ \mu^- \gamma$ events, result from the black points is taken as final. The a_μ is calculated in the same mass range to be $a_\mu^{\pi\pi, \text{LO}}(600 \sim 900 \text{ MeV}/c^2) = (368.2 \pm 2.5_{\text{stat}} \pm 3.3_{\text{sys}}) \times 10^{-10}$. Fig. 3 shows the comparison between BESIII and other measurements. Obviously, the BESIII result tends to confirm KLOE's result, but we need to keep in mind that the deviation with BaBar is only 1.7σ .



The statistical and systematic errors are added quadratically.

The band shows the 1σ range of the BESIII result.

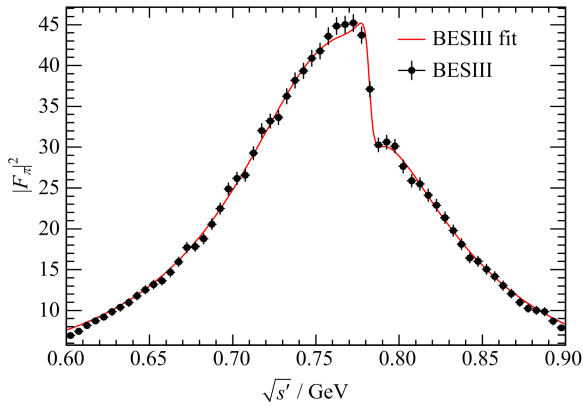
Fig. 3 Our calculation^[11] of the LO hadronic vacuum polarization 2π contributions to $(g-2)_\mu$ in the energy range 600~900 MeV/c² from BESIII and based on the data from KLOE 08^[7], 10^[8], 12^[9], and BaBar^[10], with the statistical and systematic errors

The form factor is also extracted with formula

$$|F_\pi|^2(s') = \frac{3s'}{\pi\alpha\beta_\pi^3(s')} \sigma_{\pi\pi}^{\text{dressed}}(s') \quad (2)$$

with the pion velocity $\beta(s') = \sqrt{1 - 4m_\pi^2/s'}$, the charged pion mass m_π , and the dressed cross section $\sigma_{\pi\pi}^{\text{dressed}}(s') = \sigma(e^+ e^- \rightarrow \pi^+ \pi^-)(s')$ including vacuum polarization, but corrected for FSR effects. To make a comparison with other experiments, we fit the form factor with the vector meson dominance model, where the Gunaris-Sakurai parameterization^[16] for the ρ resonances is adopted. The fitted result is shown in Fig. 4.

The fit gives $\chi^2/ndf = 49.1/56$, and the fitted parameters are listed in Tab. 1, all of which are consistent with the Particle Data Group (PDG)^[17]



Only statistical errors are shown. The red line represents the fit using the Gounaris-Sakurai parametrization.

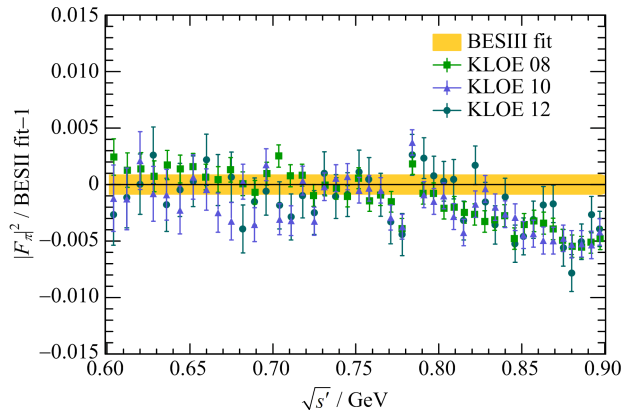
Fig. 4 The measured squared pion form factor $|F_\pi|^2$

values except the width of ρ , which shows a 3.4σ difference.

Tab. 1 Parameters and statistical errors in the Gounaris-Sakurai fit of the pion form factor

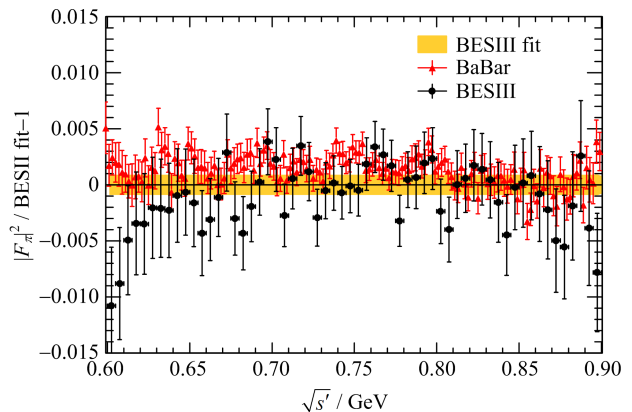
parameter	BESIII value	PDG ^[17]
$m_\rho/(\text{MeV} \cdot \text{c}^{-2})$	776.0 ± 0.4	775.26 ± 0.25
Γ_ρ/MeV	151.1 ± 0.7	147.8 ± 0.9
$m_\omega/(\text{MeV} \cdot \text{c}^{-2})$	782.1 ± 0.6	782.65 ± 0.12
Γ_ω/MeV	fixed to PDG ^[17]	8.49 ± 0.08
$ c_\omega /10^{-3}$	1.7 ± 0.2	—
$ \phi_\omega /\text{rad}$	0.04 ± 0.13	—

Comparisons with other measurements are illustrated in Figs. 5 and 6. Here, the shaded error band of the fit includes the systematic error only, while the uncertainties of the data points include the sum of the statistical and systematic errors. We observe a very good agreement with the KLOE 08 and KLOE 12 data sets up to the mass range of the $\rho-\omega$ interference. In the same mass range, the BaBar and KLOE 10 data sets show a systematic shift; however, the deviation is, within 1 to 2 standard deviations. At higher masses, the statistical error bars in the case of BESIII are relatively large, such that a comparison is not conclusive. There seems to be a good agreement with the BaBar data, while a large deviation with all three KLOE data sets is visible. There are indications that the BESIII data and BESIII fit show some disagreement in the low mass and very high mass tails as well.



Statistical and systematic uncertainties are included in the data points. The width of the BESIII band shows the systematic uncertainty only

Fig. 5 Relative difference of the form factor squared from KLOE^[7-9] and the BESIII fit



Statistical and systematic uncertainties are included in the data points. The width of the BESIII band shows the systematic uncertainty only

Fig. 6 Relative difference of the form factor squared from BaBar^[10] and the BESIII fit

2.3 Perspective of $e^+e^- \rightarrow \pi^+\pi^-\pi^0$

Many efforts have been made on the study of $e^+e^- \rightarrow \pi^+\pi^-\pi^0$ process, including both energy scan experiments and ISR analysis. Below 1.0 GeV, ω and ϕ dominate the mass spectrum, and the most precise results so far have come from energy scan experiments, like CMD2^[18-20] and SND^[21-24]. By comparing results from the two, there are still points where the difference between them is as large as 10%. Above the ϕ resonance, BaBar measured the cross section until 3.0 GeV^[25]. The discrepancy with DM2^[26] is very

large, around 1.6 GeV. All these differences need to be clarified with upcoming new results.

At BESIII, we use the 2.93 fb^{-1} data taken at the ϕ'' peak to perform an ISR study. The wide mass spectrum is expected to be measured from ω to J/ψ resonance. Compared to BaBar, the advantage is that we can benefit from both tagged and untagged methods for different mass ranges. Above 1.4 GeV, the statistics is increased significantly due to the untagged method. As a result, measurement of branching fraction $J/\psi \rightarrow \pi^+ \pi^- \pi^0$ with very high precision is feasible.

3 Conclusion

We perform a cross section measurement of the $\sigma^{\text{bare}}(e^+ e^- \rightarrow \pi^+ \pi^- (\gamma_{\text{FSR}}))$ with an accuracy of 0.9% in the dominant $\rho(770)$ mass region between 600 and 900 MeV/c^2 . The two-pion contribution to the hadronic vacuum polarization part of $(g-2)_\mu$ is determined to be $a_\mu^{\text{had,LO}}(600 \sim 900 \text{ MeV}/c^2) = (368.2 \pm 2.5_{\text{stat}} \pm 3.3_{\text{sys}}) \times 10^{-10}$. The pion form factor is extracted with vacuum polarization. It is found to be closer to KLOE's result, while the deviation with BaBar is less than 2σ . By exploiting the ISR technique, study on other channels is ongoing.

References

- [1] DAVIER M, HOECKER A, MALESCU B, et al. Reevaluation of the hadronic contributions to the muon $g-2$ and to $\alpha(M_Z^2)$ [J]. *Eur Phys J C*, 2011, 71: 1 515.
- [2] GRANGE J, GUARINO V, WINTER P, et al. Muon $(g-2)$ Technical Design Report[EB/OL]. (2015-01-27)[2015-11-30]. <http://arxiv.org/abs/1501.06858>.
- [3] BOUCHIAT C, MICHEL L. La r sonance dans la diffusion m son π m son π et le moment magn tique anormal du m son μ [J]. *J Phys Radium*, 1961 22: 121.
- [4] GOURDIN M, DE RAFAEL E. Hadronic contributions to the muon g-factor[J]. *Nucl Phys B*, 1969, 10(4): 667-674.
- [5] BRODSKY S J, DE RAFAEL E. Suggested boson-lepton pair couplings and the anomalous magnetic moment of the muon[J]. *Phys Rev*, 1968, 168(5): 1 620-1 622.
- [6] ALOISIO A, AMBROSINO F, ANTONELLI A, et al. Measurement of $\sigma(e^+ e^- \rightarrow \pi^+ \pi^- \gamma)$ and extraction of $\sigma(e^+ e^- \rightarrow \pi^+ \pi^-)$ below 1 GeV with the KLOE detector[J]. *Phys Lett B*, 2005, 606(1/2): 12-24
- [7] AMBROSINO F, ANTONELLI A, ANTONELLI M, et al. Measurement of $\sigma(e^+ e^- \rightarrow \pi^+ \pi^- \gamma(\gamma))$ and the dipion contribution to the muon anomaly with the KLOE detector[J]. *Phys Lett B*, 2009, 670(4/5): 285-291.
- [8] AMBROSINO F, ARCHILLI F, BELTRAME P, et al. Measurement of $\sigma(e^+ e^- \rightarrow \pi^+ \pi^-)$ from threshold to 0.85 GeV^2 using initial state radiation with the KLOE detector[J]. *Phys Lett B*, 2011, 700(2): 102-110.
- [9] BABUSCI D, BADONI D, BALWIERZ-PYTKO I, et al. Precision measurement of $\sigma(e^+ e^- \rightarrow \pi^+ \pi^- \gamma)/\sigma(e^+ e^- \rightarrow \mu^+ \mu^- \gamma)$ and determination of the $\pi^+ \pi^-$ contribution to the muon anomaly with the KLOE detector[J]. *Phys Lett B*, 2013, 720(4/5): 336-343.
- [10] AUBERT B, KARYOTAKIS Y, LEES J P, et al. Precise measurement of the $e^+ e^- \rightarrow \pi^+ \pi^- (\gamma)$ cross section with the initial state radiation method at BABAR[J]. *Phys Rev Lett*, 2009, 103: 231801.
- [11] ABLIKIM M, ACHASOV M N, AI X C, et al. Measurement of the $e^+ e^- \rightarrow \pi^+ \pi^-$ Cross Section between 600 and 900 MeV Using Initial State Radiation [EB/OL]. (2015-11-17)[2015-11-30]. <http://arxiv.org/abs/1507.08188>.
- [12] ABLIKIM M, AN Z H, BAI J Z, et al. Design and construction of the BESIII detector[J]. *Nucl Instrum Meth A*, 2010, 614(3): 345-399.
- [13] CZYŻ H, KÜHN J H, WAPIENIK A. Four-pion production in τ decays and $e^+ e^-$ annihilation: An update[J]. *Phys Rev D*, 2008, 77: 114005.
- [14] HOECKER A, SPECKMAYER P, STELZER J, et al. TMVA - Toolkit for Multivariate Data Analysis [EB/OL]. (2007-03-04)[2015-11-30]. <http://arxiv.org/abs/physics/0703039>.
- [15] AGOSTINELLI S, ALLISON J, AMAKO K, et al. GEANT4-a simulation toolkit[J]. *Nucl Instrum Meth A*, 2003, 506(3): 250-303.
- [16] GOUNARIS G J, SAKURAI J J. Finite-width corrections to the vector-meson-dominance prediction for $\rho \rightarrow e^+ e^-$ [J]. *Phys Rev Lett*, 1968, 21: 244.
- [17] OLIVE K A, AGASHE K, AMSLER C, et al. Review of particle physics [J]. *Chin Phys C*, 2014, 38(09): 090001.
- [18] AKHMETSHIN R R, AKSENOV G A, ANASHKIN E V, et al. Measurement of ϕ meson parameters with CMD-2 detector at VEPP-2M collider[J]. *Phys Lett B*,

- 1995, 364(3): 199-206.
- [19] AKHMETSHIN R R, AKSENOV G A, ANASHKIN E V, et al. Study of dynamics of $\varphi \rightarrow \pi^+\pi^-\pi^0$ decay with CMD-2 detector [J]. Phys Lett B, 1998, 434(3/4): 426-436.
- [20] AKHMETSHIN R R, ANASHKIN E V, AULCHENKO V M, et al. Measurement of ω meson parameters in $\pi^+\pi^-\pi^0$ decay mode with CMD-21[J]. Phys Lett B, 2000, 476(1/2): 33-39.
- [21] ACHASOV M N, AULCHENKO V M, BARU S E, et al. The process $e^+e^- \rightarrow \pi^+\pi^-\pi^0$ in the energy range $2E_0 = 1.04 \sim 1.38$ GeV [J]. Phys Lett B, 1999, 462(3/4): 365-370.
- [22] ACHASOV M N, BELOBORODOV K I, BERDYUGIN A V, et al. Measurements of the parameters of the $\varphi(1020)$ resonance through studies of the processes $e^+e^- \rightarrow K^+K^-$, $K_S K_L$, and $\pi^+\pi^-\pi^0$ [J]. Phys Rev D, 2001, 63: 072002.
- [23] ACHASOV M N, AULCHENKO V M, BELOBORODOV K I, et al. Study of the process $e^+e^- \rightarrow \pi^+\pi^-\pi^0$ in the energy region \sqrt{s} from 0.98 to 1.38 GeV [J]. Phys Rev D, 2002, 66: 032001.
- [24] ACHASOV M N, BELOBORODOV K I, BERDYUGIN A V, et al. Study of the process $e^+e^- \rightarrow \pi^+\pi^-\pi^0$ in the energy region \sqrt{s} below 0.98 GeV [J]. Phys Rev D, 2003, 68: 052006.
- [25] AUBERT B, BARATE R, BOUTIGNY D, et al. Study of the $e^+e^- \rightarrow \pi^+\pi^-\pi^0$ process using initial state radiation with BABAR [J]. Phys Rev D, 2004, 70: 072004.
- [26] ANTONELLI A, BALDINI R, BIAGINI M E, et al. Measurement of the $e^+e^- \rightarrow \pi^+\pi^-\pi^0$ and $e^+e^- \rightarrow \omega\pi^+\pi^-$ reactions in the energy interval 1.350~2.400 MeV [J]. Z Phys C, 1992, 56(1): 15-19.

(上接第 300 页)

- [25] 胡海明, 祁向荣, 黄光顺, 等. 北京谱仪 R 值测量中的初态辐射修正 [J]. 高能物理与核物理, 2001, 25(8): 701-709.
HU Haiming, QI Xiangrong, HUANG Guangshun, et al. Initial state radiative correction in R measurement at BES [J]. High Energy Physics and Nuclear Physics, 2001, 25(8): 701-709.
- [26] 胡海明, 台安, 黄光顺, 等. LUND 面积定律产生子在 R 值测量中的应用 [J]. 高能物理与核物理, 2001, 25(11): 1 035-1 043.
HU Haiming, TAI An, HUANG Guangshun, et al. Applications of LUND area law generator in R measurement [J]. High Energy Physics and Nuclear Physics, 2001, 25(11): 1 035-1 043.
- [27] 胡海明, 戴玉梅, 马凤才. LUND 面积定律对 J/ψ 非微扰强衰变的描述 [J]. 高能物理与核物理, 2003, 27(8): 673-677.
HU Haiming, DAI Yumei, MA Fengcai. Description of LUND area law to J/ψ non-perturbative hadronic decay [J]. High Energy Physics and Nuclear Physics, 2003, 27(8): 673-677.
- [28] SJÖSTRAND T. PYTHIA 5. 7 and JETSET 7. 4: Physics and Manual [R]. CERN, 1993; CERN-TH. 7112/93.